Applied Physics Letters

Dependence of the colored frequency noise in spin torque oscillators on current and magnetic field

Cite as: Appl. Phys. Lett. **104**, 092405 (2014); https://doi.org/10.1063/1.4867257
Submitted: 05 February 2014 . Accepted: 18 February 2014 . Published Online: 04 March 2014

Anders Eklund, Stefano Bonetti, Sohrab R. Sani, S. Majid Mohseni, Johan Persson, Sunjae Chung, S. Amir Hossein Banuazizi, Ezio Iacocca, Mikael Östling, Johan Åkerman, and B. Gunnar Malm

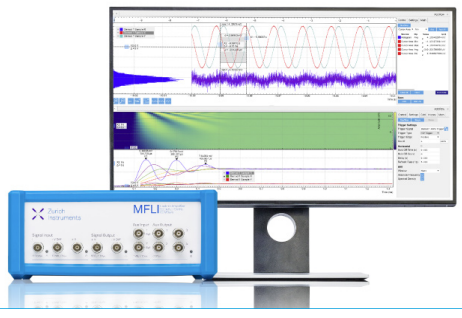

Dependence of the colored frequency noise in spin torque oscillators on current and magnetic field

Anders Eklund,[1,a)] Stefano Bonetti,[2] Sohrab R. Sani,[1] S. Majid Mohseni,[1,3] Johan Persson,[4] Sunjae Chung,[1] S. Amir Hossein Banuazizi,[1] Ezio Iacocca,[5] Mikael Östling,[1] Johan Åkerman,[1,4,5] and B. Gunnar Malm[1]

[1]*School of Information and Communication Technology, KTH Royal Institute of Technology, Electrum 229, 164 40 Kista, Sweden*
[2]*Department of Physics, Stanford University, Stanford, California 94305, USA*
[3]*Department of Physics, Shahid Beheshti University, Evin, Tehran 19839, Iran*
[4]*NanOsc AB, Electrum 205, 164 40 Kista, Sweden*
[5]*Department of Physics, University of Gothenburg, Box 100, 405 30 Gothenburg, Sweden*

(Received 5 February 2014; accepted 18 February 2014; published online 4 March 2014)

The nano-scale spin torque oscillator (STO) is a compelling device for on-chip, highly tunable microwave frequency signal generation. Currently, one of the most important challenges for the STO is to increase its longer-time frequency stability by decreasing the 1/*f* frequency noise, but its high level makes even its measurement impossible using the phase noise mode of spectrum analyzers. Here, we present a custom made time-domain measurement system with 150 MHz measurement bandwidth making possible the investigation of the variation of the 1/*f* as well as the white frequency noise in a STO over a large set of operating points covering 18–25 GHz. The 1/*f* level is found to be highly dependent on the oscillation amplitude-frequency non-linearity and the vicinity of unexcited oscillation modes. These findings elucidate the need for a quantitative theoretical treatment of the low-frequency, colored frequency noise in STOs. Based on the results, we suggest that the 1/*f* frequency noise possibly can be decreased by improving the microstructural quality of the metallic thin films. © *2014 AIP Publishing LLC*. [http://dx.doi.org/10.1063/1.4867257]

The spin torque oscillator[1–3] (STO) is a nano-scale device utilizing spin polarization of an electrical dc current to drive a steady-state magnetization precession, resulting in an oscillating voltage with a frequency in the high microwave range[4] governed by the ferromagnetic resonance (FMR) frequency. Possible applications include wide-band high-frequency communication, hard disk drive bit pattern sensing,[5] and generation of large-amplitude propagating spin waves[6,7] for magnonic devices.[8]

For any oscillator, a key parameter is its stability in terms of frequency or, equivalently, phase noise.[9] Previous work[10,11] has shown the existence of two different types of STO frequency noise, namely, 1/*f* and white, and that the frequency-domain spectrum both changes its shape and increases its linewidth as the colored, 1/*f* frequency noise becomes dominating on longer timescales.[10] The presence of white frequency noise originates from random-walk processes for the phase and has been the subject of theoretical analysis[12,13] showing that it is governed by the nontrivial amplitude-frequency relation generally seen in STOs. On the other hand, the current knowledge about the 1/*f* frequency noise is limited to the experimental determination of its existence and order of magnitude.[10] Extensive work on the STO frequency noise spectrum is hindered primarily by the inability of commercially available instruments, such as spectrum analyzers (SAs) equipped with a phase noise measurement mode, to lock on the comparatively unstable STOs. This inability in itself indicates the significance, not the least for applications, of understanding and decreasing the longer-timescale, strong 1/*f* frequency fluctuations.

In this Letter, we present a discussion of the nature of the 1/*f* frequency noise in STOs, based on measurements of its variation with the operating point (defined by the electric current and magnetic field). The investigation is made possible by the development of a custom time-domain measurement circuit providing a 150 MHz measurement bandwidth (approximately four times higher than previously achieved[10]), allowing characterization of complete sets of adjacent operating points without being limited to only the points of highest frequency stability. The detailed current dependence of the frequency noise is presented for a number of magnetic field strengths, giving rise to diverse STO frequency generation in two nominally identical samples with fundamentally different characteristics; sample A has one single oscillation mode, while sample B has two competing modes.

The samples investigated are nano-contact STOs[14] with a nominally 100 nm contact diameter, fabricated similarly to those in Refs. 15–17 and showing microwave oscillations for current densities in the order of 10^8 A/cm^2. The pseudo-spin valve stack consists of a Pd(8)/Cu(15) buffer layer, a Co(8)/Cu(6)/$Ni_{80}Fe_{20}$(4.5) giant magnetoresistance (GMR) trilayer, and a Cu(3)/Pd(3) capping layer, where all thicknesses are given in nanometers. All thin films were deposited by either rf or dc sputtering in an Ar sputtering pressure of 2.5 mTorr. The metallic layers were etched into 16 × 8 μm mesas using an Ar plasma sputter etch and were then insulated with 30 nm PECVD deposited SiO_2. The 100 nm diameter nano-contacts were defined using e-beam lithography

[a)]Electronic mail: ajeklund@kth.se

and metallized by Cu. Optical lithography and lift-off were used to deposit a 2.1 μm thick Cu top contact layer with a coplanar waveguide, leading to ground-signal-ground (GSG) connection pads. The final devices had a GMR of around 1%, and the saturation magnetization $4\pi M_s$ for the two ferromagnetic layers was determined through FMR measurements of the patterned sample to be 8.8 kG for the NiFe free layer and 18.0 kG for the Co fixed layer.

The measurements on active STOs were performed at room temperature, with magnetic field strengths H in the order of 10 kOe applied at an out-of-plane angle of 70° to excite the propagating oscillation mode[18] and maximize its power while keeping the linewidth low.[19] The devices were contacted with a 40 GHz GSG microwave probe. The dc bias current I_{dc} (sourced from a Keithley 6221) was supplied through a bias-T and the resulting ac component was fed to a 45 dB gain, 0.1–26.5 GHz low noise amplifier (LNA) with a 3.5 dB noise figure. A Rohde and Schwarz FSU 67 SA was used to determine the spectral density as a function of current for the various field strengths. The SA was swept in the 0.1–30 GHz range (15–30 GHz for sample B) utilizing a resolution bandwidth of 2 MHz, video bandwidth 10 kHz and averaging over 5 consecutive sweeps, resulting in a total acquisition time of 9.5 s for each spectrum.

Time-domain measurements of the oscillating signal were made by connecting the LNA to a microwave mixer with 5.5 dB conversion loss. Downmixing was performed to a center intermediate frequency (IF) of 75 MHz followed by amplification in a 34 dB gain, 0–500 MHz amplifier after which 128 ms long timetraces were recorded on a real-time oscilloscope with a 200 MHz bandwidth limiter and a sampling rate of 1 GS/s. A 150 MHz low-pass software filter was used to reduce high-frequency noise. This 150 MHz observation bandwidth was manually centered around the STO peak by adjusting the LO input reference frequency on the mixer.

The timetraces were processed similar to the procedure in Ref. 10. From the zero-crossing times, a nominal frequency (close to the nominal IF) was calculated and used to retrieve the phase deviation (i.e., phase noise) $\phi(t)$ at each zero-crossing. To reduce the effect of electric background measurement noise from the amplifiers (which occasionally produces false zero-crossing values), a correction algorithm was implemented to delete fast zero-crossings occurring in-between the nominal ~75 MHz crossings (a zero-crossing pair was removed whenever its frequency exceeded 220% of the IF—thus being well above the bandwidth of 150 MHz). The phase noise spectral density $S_\phi(f)$ (where f is the fluctuation frequency) was calculated over Hann windowed, half-overlapping segments of 40 and 20 ms in length. Since a linearly changing phase deviation results in an oscillation when windowed with a bell shape such as the Hann window, the lowest frequency points do not represent fluctuations in the signal; therefore, the 40 ms curves were used only to determine the valid range for the 20 ms curves (the seven lowest frequency points had to be omitted). Through the Fourier identity of the derivative, the frequency noise spectral density $S_\nu(f)$ was calculated as $S_\nu(f) = f^2 S_\phi(f)$ where

$$\nu(t) = \frac{1}{2\pi}\frac{d\phi(t)}{dt}, \tag{1}$$

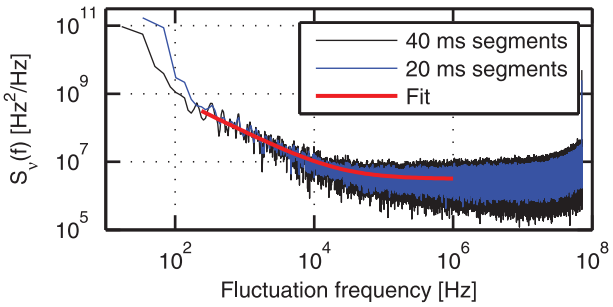

FIG. 1. Frequency noise spectral density for sample A at $H = 10.5$ kOe and $I_{dc} = 30$ mA.

is the instantaneous frequency deviation of the STO and f is the fluctuation frequency for $\nu(t)$. An example of a time segment averaged $S_\nu(f)$ is shown in Figure 1, fitted with the function

$$S_{\nu,\mathrm{fit}}(f) = S_{\nu,1/f}/f + S_{\nu,\mathrm{white}}. \tag{2}$$

The white frequency noise level $S_{\nu,\mathrm{white}}$ was extracted as the average value of $S_\nu(f)$ over $f = 0.1$–1 MHz, and this level was then used to fit an adjoining $1/f$ part to the complete range of f. The positive slope visible above 20 MHz in Figure 1 has the same level for all operating points and represents the white phase noise measurement floor of the setup. The plots of $S_{\nu,1/f}$ and $S_{\nu,\mathrm{white}}$ in Figures 2 and 3 display the mean and standard deviation for fits made for each individual 20 ms segment. Data points are displayed for the current regions where the signal-to-noise ratio (SNR) was good and the $S_\nu(f)$ spectrum uncompromised; for worse SNR, $S_{\nu,\mathrm{white}}$ tended to go up (significantly above the maximum $\pi S_{\nu,\mathrm{white}}$ level indicated by the SA linewidth) as also verified numerically and experimentally using a commercial signal generator connected to the LNA. The same inability to extract correct zero-crossings in too low SNR at the same time resulted in decreased $S_{\nu,1/f}$ levels.

Figure 2 shows the power spectral density, SA Lorentzian fitted linewidth Δf (full width at half maximum, FWHM), and $\pi S_{\nu,\mathrm{white}}$ and $S_{\nu,1/f}$ of sample A as a function of I_{dc} for three magnetic field strengths. In the absence of other frequency noise types, $S_{\nu,\mathrm{white}}$ would produce a frequency-domain Lorentzian with a linewidth of $\pi S_{\nu,\mathrm{white}}$,[10] allowing a direct comparison (in the same units) with the SA linewidth Δf. As can be seen in Figures 2(d)–2(f), the STO linewidth as measured with the SA is generally well explained by the white frequency noise alone.

The qualitative and quantitative correspondence further strengthens the previous observations[12,20,21] of the correlation between the linewidth (i.e., $\pi S_{\nu,\mathrm{white}}$) and the nonlinear amplification factor (coincidently also denoted ν) of the general nonlinear auto-oscillator theory[22] of the STO, calculated by the means of Ref. 21. We noted that both the nonlinear amplification factor and $(df/dI_{dc})^2$ (as suggested in Ref. 23 to have impact on the frequency noise) look very similar and agree qualitatively with the shape of the linewidth and $\pi S_{\nu,\mathrm{white}}$ versus I_{dc} curves. An exhaustive investigation of this topic is, however, outside the scope of this Letter.

Noise in the dc current source as an origin for the frequency noise was ruled out in an additional measurement in a

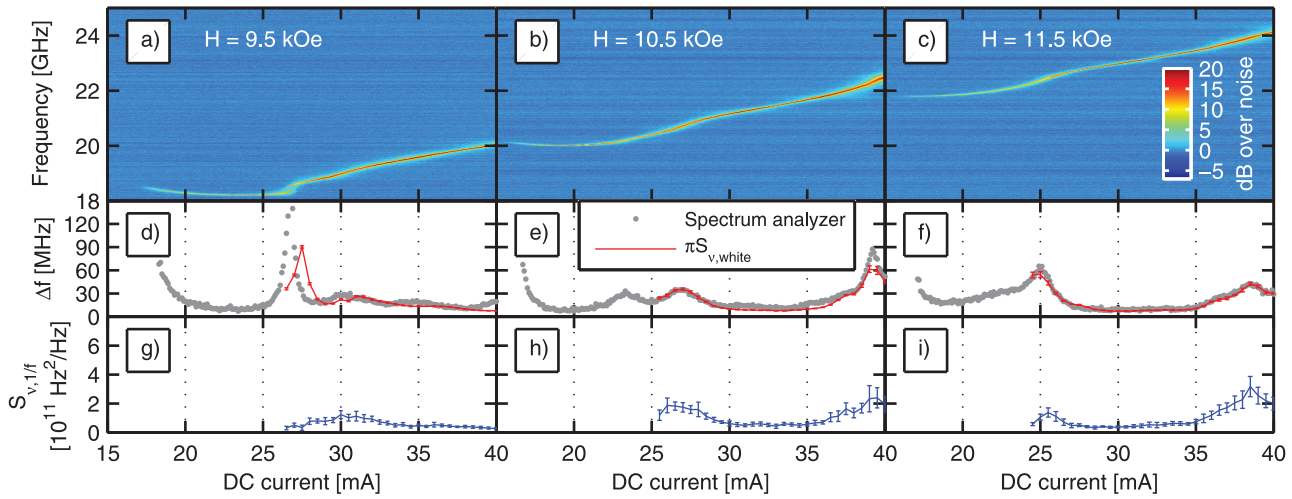

FIG. 2. (a)–(c) Power spectral density and (d)–(i) frequency noise for sample A in (a), (d), and (g) $H = 9.5$ kOe; (b), (e), and (h) $H = 10.5$ kOe; and (c), (f), and (i) $H = 11.5$ kOe.

sample with lower threshold current (increased current density by using a thicker bottom Cu layer to decrease current spreading within the GMR films), where the range setting of the dc current source could be changed from 100 mA to 20 mA. Although this operation decreases the noise in I_{dc} by 5–10 dB, no change in the STO frequency stability was observed.

Noise in the magnetic field, generated by our electromagnet, could also be ruled out; the experimentally determined $(df/dH)^2$ did not convincingly correspond qualitatively to the peaks and valleys of the frequency noise (as a function of current), and a measurement performed with a 9.37 kOe permanent Halbach array magnet showed neither a qualitative difference nor an order-of-magnitude change in any of the frequency noise quantities.

Regarding the $1/f$ frequency noise in Figures 2(g)–2(i), it is *not* a monotonic function of I_{dc}. Moreover, it changes as a function of the magnetic field strength in a way similar to the SA linewidth and $\pi S_{\nu,\mathrm{white}}$. Nor is it a function of the oscillation frequency, as for example can be seen by comparing the I_{dc} ranges of minimum $S_{\nu,1/f}$. This nearly identical minimum value ($S_{\nu,1/f} \approx 0.5 \times 10^{11}$ Hz^2/Hz) is obtained within 19.5–20.0, 21.0–21.7, and 22.7–23.4 GHz for the respective field strengths. In conclusion, the $1/f$ noise behavior for single-mode oscillation can best be described as a function of the frequency-I_{dc} nonlinearity—which also governs the white frequency noise.

The multi-mode sample B (Figure 3) shows qualitatively different frequency noise behavior for $I_{dc} \geq 34.0$ mA. For $I_{dc} < 34.0$ mA in both field strengths 10.5 and 11.5 kOe, the SA linewidth, $\pi S_{\nu,\mathrm{white}}$ and $S_{\nu,1/f}$ (Figures 3(c)–3(f)), show trends similar to those of sample A (with the exception of a lower peak value for $S_{\nu,1/f}$ and an uncorrelated rise towards 34.0 mA in Figure 3(e)). However, for $I_{dc} \geq 34.0$ mA, 10.5 kOe in Figure 3(a) we see an onset of a higher-frequency mode, approximately 1 GHz above the original mode. While this new mode had too weak oscillation amplitude to be observed in the time-domain, our measurements of the original mode (Figures 3(g)–3(i), also marked in Figure 3(a)) show a stochastic ON/OFF-switching within the 150 MHz measurement bandwidth. The noncontinuous waveform prevents a meaningful extraction of the frequency noise spectrum; however, we observe increasing ON/OFF-switching rates as a

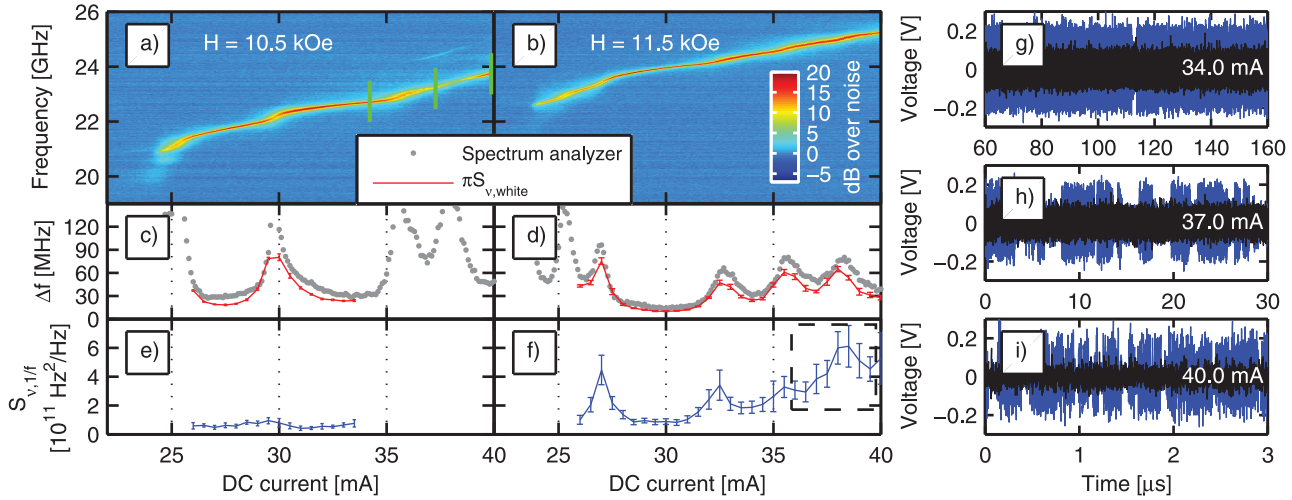

FIG. 3. (a) and (b) Power spectral density and (c)–(f) frequency noise for sample B in (a), (c), and (e) $H = 10.5$ kOe and (b), (d), and (f) $H = 11.5$ kOe. Recorded timetraces at $H = 10.5$ kOe for the lower-frequency, dominating mode (blue) and background at $I_{dc} = 0$ mA (black) for (g) 34.0 mA, (h) 37.0 mA, and (i) 40.0 mA. The higher-frequency mode is outside the 150 MHz bandwidth.

function of bias current, in agreement with the increase of thermal spin-wave coupling channels recently suggested analytically.[24,25] The involved timescale ranges from hundreds of μs for Figure 3(g) to sub-μs for Figure 3(i). Although the higher-frequency mode voltage amplitude was too weak to be observed in the time-domain for sample B, in Ref. 26, a similar behavior was found in similar operating conditions for a similar device and it was unambiguously observed that the STO was constantly jumping between the involved frequencies. As the magnetic field strength is increased, the higher-frequency mode disappears from the spectrum and at 11.5 kOe (Figure 3(b)) the time-domain waveform of the main mode is once again continuous. However, in the high-current region of the non-excited second mode, the 1/*f* noise shows an elevated level (highlighted section of Figure 3(f)), both compared to the previous values and to the behavior of $\pi S_{\nu,\mathrm{white}}$ in Figure 3(d).

Although the observed 1/*f* frequency noise slope in all our measurements might in theory represent the high-frequency tail of longer correlations, we found no such indication down to our lower measurement limit of $\sim$100 Hz. Therefore, in the following three paragraphs, we will discuss the potential origin of the observed pure 1/*f* noise.

As seen in both sample A and the single-mode region of sample B, the 1/*f* frequency noise for single-mode oscillation appears to be correlated to the same nonlinear amplification factor between amplitude noise and frequency noise as has been analytically identified for white frequency noise,[12] or to $(df/dI_{\mathrm{dc}})^2$. The origin of this possible 1/*f* noise in the oscillation amplitude is not as clear as in the case of the white, thermally generated noise. We suggest that it may come from long-term weakly chaotic[27] magnetization trajectories; the oscillation trajectory may not necessarily be a perfect limit cycle. In this case, the 1/*f* noise is inherent to the precession dynamics and not easily improved. Another possibility concerns 1/*f* magnetoresistive noise in the sputtered magnetic thin films of GMR spin valves;[28] it is natural to envisage how 1/*f* magnetoresistive noise can give rise to 1/*f* noise in the spin torque and thereby in the magnetization oscillation amplitude. In Ref. 28, this magnetoresistive noise is found to be "associated with fluctuations in the magnetic microstructure having a length scale set by the disorder formed during the deposition and processing of the materials stack"—e.g., metallic grains originally formed in the sputtering process. This suggests that the 1/*f* amplitude noise and thereby the 1/*f* frequency noise could potentially be decreased by improving the microstructural quality of the deposited films.

The behavior of $S_{\nu,1/f}$ at high currents for sample B suggests that the second, higher-frequency mode continues to influence the magnetization precession also at operating points where it is no longer properly excited. In this sense, the "background" mode can induce longer correlations due its vanishing yet finite energy,[25] leading to increased white and 1/*f* noise. With this interpretation, the gradual increase in $S_{\nu,1/f}$ in Figure 3(e) for $31.0\,\mathrm{mA} < I_{\mathrm{dc}} \leq 34.0\,\mathrm{mA}$ before the time-domain observed onset of the higher-frequency mode (an increase which does not occur for $\pi S_{\nu,\mathrm{white}}$) is a fully natural observation as the higher-frequency mode approaches excitability along the I_{dc} instead of the H dimension in the parameter space.

The "background" mode effect could potentially be depleted by controlling the number of available modes to a single one. Two recent studies[29,30] have shown that the generated frequency is highly dependent on the in-plane angle and even polarity of the applied magnetic field, leading to reasoning about spatial microstructural film inhomogeneity as the cause. It is not unlikely that the presence of several frequencies in sample B is related to different areas of the films underneath the nano-contact alternately dominating the magnetization precession. Therefore, we expect that increased film deposition quality would decrease the number of modes and therefore also decrease the influence of "background" modes on the 1/*f* frequency noise.

In conclusion, by using a 150 MHz wide microwave down-mixing, time-domain technique, we have found that the colored, 1/*f* frequency noise in GMR nano-contact spin torque oscillators is closely related to the I_{dc}-frequency nonlinearity in a way similar to that of the white frequency noise and the spectrum FWHM linewidth. We have also observed that the nearby (in parameter space) existence of an unexcited alternative precession mode can act to increase the 1/*f* level. Based on these results, we propose that improvement of the sputtered film quality may have a significant positive effect on the 1/*f* frequency noise.

This work was supported by the Swedish Foundation for Strategic Research (SSF), the Swedish Research Council (VR) under Contract No. 2009-4190, and the Knut and Alice Wallenberg Foundation (KAW). Johan Åkerman is a Royal Swedish Academy of Sciences Research Fellow supported by a grant from KAW.

[1]J. Slonczewski, J. Magn. Magn. Mater. **159**, L1 (1996).
[2]L. Berger, Phys. Rev. B **54**, 9353 (1996).
[3]J.-V. Kim, in *Solid State Physics*, edited by R. E. Camley and R. L. Stamps (Academic Press, 2012), Vol. 63, pp. 217–294.
[4]S. Bonetti, P. Muduli, F. Mancoff, and J. Åkerman, Appl. Phys. Lett. **94**, 102507 (2009).
[5]R. Sato, K. Kudo, T. Nagasawa, H. Suto, and K. Mizushima, IEEE Trans. Magn. **48**, 1758 (2012).
[6]M. Madami, S. Bonetti, G. Consolo, S. Tacchi, G. Carlotti, G. Gubbiotti, F. B. Mancoff, M. A. Yar, and J. Åkerman, Nat. Nanotechnol. **6**, 635 (2011).
[7]V. E. Demidov, S. Urazhdin, and S. O. Demokritov, Nature Mater. **9**, 984 (2010).
[8]V. V. Kruglyak, S. O. Demokritov, and D. Grundler, J. Phys. D: Appl. Phys. **43**, 264001 (2010).
[9]M. W. Keller, A. B. Kos, T. J. Silva, W. H. Rippard, and M. R. Pufall, Appl. Phys. Lett. **94**, 193105 (2009).
[10]M. W. Keller, M. R. Pufall, W. H. Rippard, and T. J. Silva, Phys. Rev. B **82**, 054416 (2010).
[11]M. Quinsat, D. Gusakova, J. F. Sierra, J. P. Michel, D. Houssameddine, B. Delaet, M.-C. Cyrille, U. Ebels, B. Dieny, L. D. Buda-Prejbeanu, J. A. Katine, D. Mauri, A. Zeltser, M. Prigent, J.-C. Nallatamby, and R. Sommet, Appl. Phys. Lett. **97**, 182507 (2010).
[12]J.-V. Kim, V. Tiberkevich, and A. N. Slavin, Phys. Rev. Lett. **100**, 017207 (2008).
[13]T. Silva and M. W. Keller, IEEE Trans. Magn. **46**, 3555 (2010).
[14]T. Silva and W. Rippard, J. Magn. Magn. Mater. **320**, 1260 (2008).
[15]R. K. Dumas, E. Iacocca, S. Bonetti, S. R. Sani, S. M. Mohseni, A. Eklund, J. Persson, O. Heinonen, and J. Åkerman, Phys. Rev. Lett. **110**, 257202 (2013).
[16]S. R. Sani, J. Persson, S. M. Mohseni, V. Fallahi, and J. Åkerman, J. Appl. Phys. **109**, 07C913 (2011).
[17]S. M. Mohseni, S. R. Sani, J. Persson, T. N. A. Nguyen, S. Chung, Y. Pogoryelov, P. K. Muduli, E. Iacocca, A. Eklund, R. K. Dumas, S. Bonetti, A. Deac, M. A. Hoefer, and J. Åkerman, Science **339**, 1295 (2013).

[18]J. Slonczewski, J. Magn. Magn. Mater. **195**, L261 (1999).
[19]S. Bonetti, V. Puliafito, G. Consolo, V. S. Tiberkevich, A. N. Slavin, and J. Åkerman, Phys. Rev. B **85**, 174427 (2012).
[20]B. Georges, J. Grollier, V. Cros, A. Fert, A. Fukushima, H. Kubota, K. Yakushijin, S. Yuasa, and K. Ando, Phys. Rev. B **80**, 060404 (2009).
[21]P. K. Muduli, O. G. Heinonen, and J. Åkerman, Phys. Rev. B **86**, 174408 (2012).
[22]A. Slavin and V. Tiberkevich, IEEE Trans. Magn. **45**, 1875 (2009).
[23]W. H. Rippard, M. R. Pufall, and S. E. Russek, Phys. Rev. B **74**, 224409 (2006).
[24]O. Heinonen, Y. Zhou, and D. Li, "Mode coupling in spin torque oscillators," Phys. Rev. B (submitted); e-print arXiv:1310.6791.
[25]E. Iacocca, O. Heinonen, P. K. Muduli, and J. Åkerman, Phys. Rev. B **89**, 054402 (2014).
[26]A. J. Eklund, S. R. Sani, S. M. Mohseni, J. Persson, B. G. Malm, and J. Åkerman, "Triple mode-jumping in a spin torque oscillator," in *22nd International Conference on Noise and Fluctuations (ICNF)* (IEEE, 2013).
[27]Z. Li, Y. C. Li, and S. Zhang, Phys. Rev. B **74**, 054417 (2006).
[28]Z. Diao, E. R. Nowak, K. M. Haughey, and J. M. D. Coey, Phys. Rev. B **84**, 094412 (2011).
[29]S. Tamaru and D. Ricketts, IEEE Magn. Lett. **3**, 3000504 (2012).
[30]M. R. Pufall, W. H. Rippard, S. E. Russek, and E. R. Evarts, Phys. Rev. B **86**, 094404 (2012).